Materials Research Proceedings 42 (2024) 121-125 https://doi.org/10.21741/9781644903193-27

Wing-aileron adaptive flutter suppression system

Carmelo Rosario Vindigni[1,a *], Calogero Orlando[1,b], Antonio Esposito[1,c] and Andrea Alaimo[1,d]

[1]Kore University of Enna, M.A.R.T.A. Centre, Enna, 94100, Italy

[a]carmelorosario.vindigni@unikore.it, [b]calogero.orlando@unikore.it, [c]antonio.esposito@unikore.it, [d]andrea.alaimo@unikore.it

Keywords: Wing Aileron Stick Model, Flutter Suppression, Simple Adaptive Control

Abstract. In this work a flutter suppression system design based on simple adaptive control architecture and an alternative beam finite element modelling of wings equipped with trailing edge control surfaces is proposed. The aeroelastic beam finite element used is based on Euler-Bernoulli beam theory for the flexural behavior, De Saint Venant theory for torsion and two-dimensional time-domain unsteady aerodynamics applied by means of strip theory assumptions. The finite element modeling used allows to write the aero-servo-elastic plant governing equations in state-space form, from which the flutter suppression system design can be carried out in a time domain fashion. The simple adaptive control architecture has been applied to the aero-servo-elastic plant which passivity requirement has been enforced implementing a parallel feed-forward compensator.

Introduction

Over the years, wing structures design has been influenced by the preference of realizing lightweight structural configurations; however, this choice have led to face the problem of structural susceptibility to aeroelastic instabilities [1]. An open research field deals with active suppression approaches that are related to control systems implementation and actuation methods in order to stave off the instabilities by suppressing the related vibration. Flutter suppression systems design based on equivalent beam modelling of the aeroelastic plant have been studied in literature following different approaches, but the implementation of Simple Adaptive Control SAC architecture in this framework has not been explored yet. In fact, the SAC scheme has been successfully applied in literature for the flutter suppression of three degrees of freedom 3DOF airfoil models; in detail, in [2] an Implicit Reference Model IRM based SAC architecture has been developed, in [3] a SAC algorithm is used to suppress the flutter vibration of a 3DOF airfoil with pitch stiffness non-linearity, where the trailing edge control surface is deployed by means of a piezoelectric actuator, increasing the flutter boundary of about the 213% with respect to the open loop case, and the robustness of this latter aero-servo-elastic plant is studied for structural, aerodynamics, actuator, and free-play uncertainties. However, the 3DOF airfoil is a low fidelity model not representative of wings with locally distributed control surfaces; therefore, this work aims to assess the performances of the SAC flutter suppression scheme when applied to a more realistic aeroelastic plant such as the one obtained implementing an equivalent beam system.

Problem statement and finite element formulation

The aeroelastic system considered in this work is a cantilever wing with semi-span length l_w, straight elastic axis EA, and a trailing edge aileron-like control surface that extends from a distance l_F by the root to the wing tip. The aileron control surface is hinged to the wing frame; the links between the servo and the aileron hinge are also taken into account and their positions with respect to the l_F wing station are defined as l_{a1} and l_{a2}. The control surface is flexible in torsion and with elastic axis close enough to the hinge line such that they could be considered coincident. The wing is modelled as an equivalent beam according to Euler-Bernoulli and De Saint Venant beam theories

Materials Research Proceedings 42 (2024) 121-125 https://doi.org/10.21741/9781644903193-27

assumptions. The structural degrees of freedom of the wing-stick model are the vertical displacement due to bending $w(x, t)$ (positive upwards), the elastic torsional rotation $\phi(x, t)$ around the elastic axis (positive nose-up), and the control surface rotation $\delta(x, t)$ about its hinge (positive aileron down). The wing's parameters are shown in Figure 1. In detail, b is the semi-chord, a is the non-dimensional distance from the mid-chord to the elastic axis (positive aft), x_ϕ is the non-dimensional distance between the mid-chord and the center of gravity (positive aft), c identifies the control surface hinge location behind the mid-chord, while its center of gravity lies at x_δ behind the hinge.

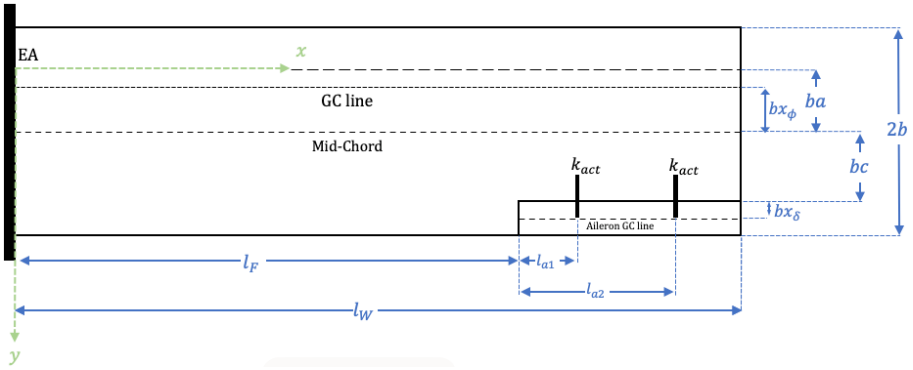

FIGURE 1: Wing-aileron schematic

The wing governing equations are the ones of a beam with bending and torsion degrees of freedom to which is added the torsional equation of motion of the aileron. A compact matrix representation of the governing equations can be obtained properly defining the structural and aerodynamic matrices that represent mass $\mathbf{M}_s$, $\mathbf{M}_{aer}$, damping $\mathbf{C}_s$, $\mathbf{C}_{aer}$, and stiffness $\mathbf{K}_s$,$\mathbf{K}_{aer}$ contributions, where the subscripts s and aer stand for structural and aerodynamic, respectively. Moreover, the gust loads contribution is introduced as $\mathbf{F}^g w_g(t)$. Thus, defining a generalized displacement vector $\mathbf{q}(t) = [w \quad \phi \quad \delta \quad \bar{x}]^T$ the governing equations compact form reads as

$$[\mathbf{M}_s + \mathbf{M}_{aer}]\ddot{\mathbf{q}}(t) + [\mathbf{C}_s + \mathbf{C}_{aer}]\dot{\mathbf{q}}(t) + [\mathbf{K}_s D^2 + \mathbf{K}_\delta + \mathbf{K}_{aer}]\mathbf{q}(t) = \mathbf{F}_g w_g(t) \tag{1}$$

where $\boldsymbol{D}$ is a differential operator related to the derivatives along the beam axis and $\mathbf{K}_\delta$ is the aileron stiffness matrix that collects the hinge and actuator stiffnesses. The matrices full expressions can be found in [4]. Introducing the displacement field interpolation and writing eq. 1 in weak form the aeroelastic beam elemental mass, damping and stiffness matrices are obtained performing the following integrals

$$\mathbf{M}_e = \int_L \mathbf{N}^T[\mathbf{M}_s + \mathbf{M}_{aer}]\mathbf{N}dx;\ \mathbf{C}_e = \int_L \mathbf{N}^T[\mathbf{C}_s + \mathbf{C}_{aer}]\mathbf{N}dx;\ \mathbf{K}_e = \int_L [(\boldsymbol{DN})^T\mathbf{K}_s\boldsymbol{D} + \mathbf{N}^T\mathbf{K}_\delta + \mathbf{N}^T\mathbf{K}_{aer}]\mathbf{N}\mathbf{dx} \tag{2}$$

Then, assembling the matrices opportunely, in accordance with the wing discretization, and imposing the boundary conditions, the structural equations of motion reads as

$$\begin{bmatrix}\mathbf{M_{11}} & \mathbf{M_{12}} \\ \mathbf{M_{12}}^T & \mathbf{M_{22}}\end{bmatrix}\begin{bmatrix}\ddot{\Delta}_1 \\ \ddot{\Delta}_2\end{bmatrix} + \begin{bmatrix}\mathbf{C_{11}} & \mathbf{C_{12}} \\ \mathbf{C_{12}}^T & \mathbf{C_{22}}\end{bmatrix}\begin{bmatrix}\dot{\Delta}_1 \\ \dot{\Delta}_2\end{bmatrix} + \begin{bmatrix}\mathbf{K_{11}} & \mathbf{K_{12}} \\ \mathbf{K_{12}}^T & \mathbf{K_{22}}\end{bmatrix}\begin{bmatrix}\Delta_1 \\ \Delta_2\end{bmatrix} = \begin{bmatrix}\mathbf{F}_S^g \\ \mathbf{0}\end{bmatrix} w_g \tag{3}$$

where Δ_1 and Δ_2 are the unknown and known displacements vectors, from which the rearrangement of the structure matrices is performed, while $\mathbf{F}_S^g w_g$ is the global gust force vector. Then, eq. 3 can be cast in state space form introducing the state vector $X = [\Delta_1^T \quad \dot{\Delta}_1^T]^T$, that collects the unknown structural displacements and their time derivative, and the dynamic matrix computed as follows

Materials Research Proceedings 42 (2024) 121-125 https://doi.org/10.21741/9781644903193-27

$$\mathbf{A} = \begin{bmatrix} 0 & I \\ -\mathbf{M}_G^{-1}\mathbf{K}_G & -\mathbf{M}_G^{-1}\mathbf{C}_G \end{bmatrix} \quad (4)$$

Moreover, in order to obtain the state-input relation **B**, a submatrix $\mathbf{K}_{12}^{\delta}$ of $\mathbf{K}_{12}$, corresponding to the aileron displacement at the actuator-aileron linking stations, must be identified. The **B** matrix is computed considering the aileron stiffness only since the related mass and damping contributions have shown to be negligible for the aileron dynamics in correspondence of the actuators. Thus, the state-input matrix and the state input relation for the gust loads read as

$$\mathbf{B} = \begin{bmatrix} \mathbf{0} \\ -\mathbf{M_{11}}^{-1}\mathbf{K}^{\delta}{}_{\mathbf{12}} \end{bmatrix}; \mathbf{B}^{g} = \begin{bmatrix} \mathbf{0} \\ -\mathbf{M_{11}}^{-1}\mathbf{F}_S^{g} \end{bmatrix} \quad (5)$$

Last, the state-output matrix **C** is an identity matrix in the hypothesis of ideal sensors; therefore, the wing state space system read as

$$\begin{cases} \dot{X} = \mathbf{A}X + \mathbf{B}u + \mathbf{B}^{g}w_g \\ Y = \mathbf{C}X \end{cases} \quad (6)$$

where u is the control input, i.e. the aileron displacement at the actuators stations, and w_g is the gust profile.

Adaptive controller

The SAC, that could be defined as a modification of the Model Reference Adaptive Control, takes into account a reference model that generates the signal to be tracked by the controlled plant in order to let it follow the desired dynamics [5].In detail, the SAC control signal is a linear combination of the reference model state, input, and of the tracking error $e(t)$; however,in this work the control objective is to make the wing tip torsion angle zeroed, thus the SAC control law is reduced to [6] taking into account the output signal $e(t) = 0 - \phi(l_w, t)$, only. Thus, the output feedback adaptive control law reads as

$$\mathrm{u(t)} = (K_{eP} + K_{eI})e(t) \quad (7)$$

where K_{eP} and K_{eI} are the controller adaptive gains expressed as $K_{eP} = \Gamma_{eP}e^2$ and $\dot{K}_{eI} + \eta K_{eI} = \Gamma_{eI}e^2$, with $\Gamma_{eP}$and Γ_{eI} invariant gains of the control algorithm and η the Iannou term that ensures the stability of the system when bounded disturbances are present [6]. However, it is to be said that the SAC algorithm can be only applied to systems that fulfill the passivity requirements [7]. In this work, a Parallel Feedforward Compensator PFC is added to the plant $G(s)$, i.e the Single Input Single Output SISO transfer function related to Eq. 6, in order to make the system meet the Almost Strictly Positive Realness ASPR condition [8]. As presented in [9], the PFC is designed as the inverse of a controller $H(s)$ that stabilize the closed loop system given by $G_c(s) = (1 + G(s)H(s))^{-1}G(s)$. The selected controller $H(s)$ is a ideal Proportional-Derivative PD controller with transfer function $H(s) = K_H(1 + \tau_H s)$, being $K_H = 3$ and $\tau_H = 10^{-3}s$, that makes the augmented plant satisfy the ASPR condition for every speed values below the SAC closed loop system flutter boundary $v_f^{SAC} = 171\ m/s$. A scheme of the SAC control architecture specialized for the wing-aileron flutter suppression is shown in Figure 2.

Materials Research Proceedings 42 (2024) 121-125 https://doi.org/10.21741/9781644903193-27

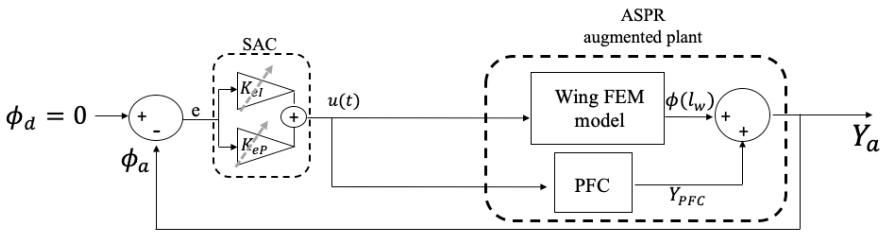

FIGURE 2: Wing-aileron SAC flutter suppression architecture

The invariant gains of the adaptive controller, namely $[\Gamma_{eP} \quad \Gamma_{eI} \quad \eta]$, are tuned using a Population Decline Swarm Optimization P_DSO algorithm [10] and considering the plant at the open loop flutter speed $v_f^{OL} = 109.5\, m/s$ subjected to a pulse disturbance on the tip torsion rate with amplitude $\dot{\phi}(l_w, 0) = 100\, rad/s$ occurring at time instant $t = 0$ and with width $t = 0.001s$. From the results of the optimization, the invariant gains are selected as $[3.046 \times 10^6 \quad 304 \quad 10^{-3}]$ providing for the minimum objective function value $ITAE_{min} = 3.71 \times 10^{-5}\, rad * s$.

Closed loop system analysis

Numerical simulations are carried out to study the performances of the SAC flutter suppression system in flight scenarios of interest where the wing is perturbed by discrete atmospheric gusts. In detail, in order to be confident with real flight scenarios, a 1−cosine discrete gust profile has been considered, as suggested by references [11,12]. One case study considered involves the wing flying at the flutter speed and simultaneously encountering a pulse disturbance on the tip torsion rate and a 1−cosine gust with maximum peak $w_{max} = 1\, m/s$ and gust semi-width $t_g = 0.25$. The simulation results are reported in Figure 3 where it can be observed that the flutter oscillations are suppressed in less that 2 seconds and kinematic variables peak values are reduced, with respect to the open loop case, with a maximum aileron deflection of 0.8deg. In detail, the tip torsion is reduced from −0.54deg to −0.43deg and the tip deflection from 0.037m to 0.028m.

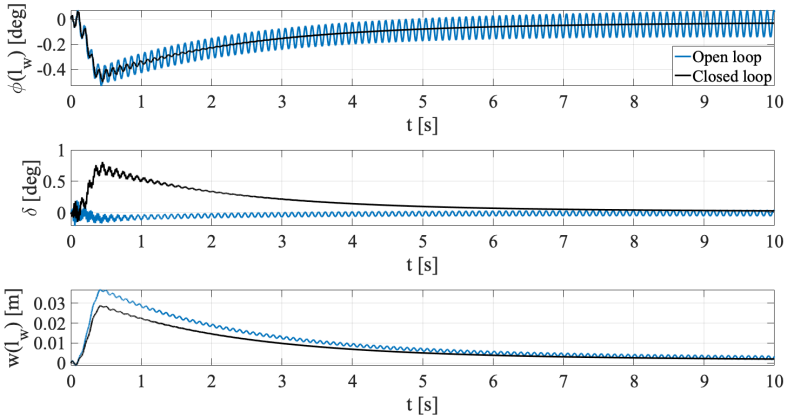

FIGURE 3: System response at the flutter speed with gust disturbance

Conclusions

This work has presented an alternative aeroelastic beam finite element method for the numerical modeling of wing structures with aileron-like control surfaces. The numerical model generated offers a suitable state space description of the aeroelastic system and has been tailored for flutter suppression system design objectives. The Adaptive Controller's invariant gains have been tuned using a meta-heuristic swarm technique called P_DSO. The adaptive flutter suppression system designed has demonstrated the ability to increase the wing flutter boundary by the 55.25%.

Numerical simulations in the presence of gust disturbance have been used to examine the performance of the closed loop system that have shown a satisfactory dynamic behavior.

Funding
The study was financially supported by the Italian Ministry of University and Research - M.U.R. under the DAVYD project (P.O.N. Grant ARS01_00940).

References

[1] E. Livne, Aircraft active flutter suppression: State of the art and technology maturation needs. *Journal of Aircraft*, *55*(1), 410-452, 2018.

[2] B. Andrievsky, E. V. Kudryashova, N. V. Kuznetsov, O. A. Kuznetsova, and G. A. Leonov, "Simple adaptive control for airfoil flutter suppression," Mathematics in Engineering, Science and Aerospace, vol. 9, no. 1, pp. 5–20, 2018.

[3] C. R. Vindigni, A. Esposito, and C. Orlando, "Stochastic aeroservoelastic analysis of a flapped airfoil," Aerospace Science and Technology, vol. 131, p. 107967, 2022.

[4] C. R. Vindigni, G. Mantegna, A. Esposito, C. Orlando, and A. Alaimo, "An aeroelastic beam finite element for time domain preliminary aeroelastic analysis," Mechanics of Advanced Materials and Structures, pp. 1–9, 2022.

[5] I. Barkana, "Simple adaptive control–a stable direct model reference adaptive control methodology–brief survey," International Journal of Adaptive Control and Signal Processing, vol. 28, no. 7-8, pp. 567–603, 2014.

[6] A. L. Fradkov, I. V. Miroshnik, and V. O. Nikiforov, Nonlinear and adaptive control of complex systems, vol. 491. Springer Science & Business Media, 2013.

[7] I. Barkana, "Robustness and perfect tracking in simple adaptive control," International Journal of Adaptive Control and Signal Processing, vol. 30, no. 8-10, pp. 1118–1151, 2016.

[8] I. Rusnak and I. Barkana, "Spr and aspr untangled," IFAC Proceedings Volumes, vol. 42, no. 6, pp. 126–131, 2009.

[9] C. R., Vindigni, G. Mantegna, C. Orlando, and A. Alaimo, Simple adaptive wing-aileron flutter suppression system. *Journal of Sound and Vibration*, *570*, 118151, 2024.

[10] Vindigni, C. R., & Orlando, C. (2020). A gain scheduling control of incompressible airfoil flutter tuned by the population decline swarm optimizer—PDSO. Aerotecnica Missili & Spazio, 99(1), 3-16.

[11] R. L. Bisplinghoff and H. Ashley, Principles of aeroelasticity. Courier Corporation, 2013.

[12] Dowell, Earl H., *A modern course in aeroelasticity*. Vol. 264. Springer Nature, 2021.